

Surface-functionalized Hexagonal Mesoporous Silica Supported 5-(4-Carboxyphenyl)-10,15,20-triphenyl Porphyrin Manganese(III) Chloride and Their Catalytic Activity

Wei-jie Zhang, Ping-ping Jiang,* Ping-bo Zhang, Jia-wei Zheng, and Haiyang Li

The Key Laboratory of Food Colloids and Biotechnology, Ministry of Education, School of Chemical and Material Engineering, Jiangnan University, Wuxi 214122, P.R. China. *E-mail: ppjiang@jiangnan.edu.cn

Received July 17, 2012, Accepted September 12, 2012

Manganese(III) 5-(4-carboxyphenyl)-10,15,20-triphenyl porphyrin chloride (Mn(TCPP)Cl) was grafted through amide bond on silica zeolite Y (HY), zeolite beta (H β) and hexagonal mesoporous silica (HMS). XRD, ICP-AES, N₂ physisorption, SEM, TEM, FTIR and thermal analysis were employed to analyse these novel heterogeneous materials. These silica supported catalysts were shown to be used for epoxidation and good shape selectivity was observed. The effect of support structure on catalytic performance was also discussed. The catalytic activity remained when the catalysts were recycled five times. The energy changes about epoxidation of alkenes by NaIO₄ and H₂O₂ were also computationally calculated to explain the different catalytic efficiency.

Key Words : Manganese(III) porphyrin, Epoxidation, HMS, Alkenes, Fatty acid

Introduction

Epoxidation of unsaturated compounds is a widely used process in the chemical industry. These epoxides are valuable intermediates for chemical manufacturing as well as laboratory synthesis, as they can be transformed into a large variety of compounds due to their high reactivity of oxirane ring. Moreover, green epoxidation of vegetable renewable source has attracted more and more interest. Epoxy long-chain unsaturated compounds were produced at industrial scale mainly by the conventional performic acid process. Long-chain olefins and unsaturated fatty acid derivatives of vegetable oils such as soybean, linseed, rapeseed, olive, corn, safflower, melon seed, and cotton seed have been widely used on an industrial scale. These substrates were sensitive to reaction condition and selectivity was usually lower. Methyl oleate and soybean oil obtained from renewable raw materials could be used for making green product such as plasticizers and stabilizers in poly(vinyl chloride) (PVC) because of its safety and innocuity.¹⁻³ Epoxy product was produced mainly by the conventional performic acid process. The separation of catalyst, whose presence may be detrimental for further applications, is not easy. In order not to lose the benefits represented by exploitation of renewable raw materials, it is worth looking for an alternative epoxidation path.

Since 1980s, synthetic metalloporphyrin has been utilized by many researchers in olefin epoxidation to mimic cytochrome P-450. However, these metalloporphyrins as homogeneous catalysts have some disadvantages. Traditional metalloporphyrin-catalyzed epoxidations are homogeneous reactions due to their soluble and degradable characteristics. It can be overcome by immobilising metalloporphyrins to insoluble solid supports. Oxides⁴⁻⁶ or organic polymers⁷⁻¹¹ in recent years have been carried out in order to obtain epoxi-

dation systems and mimic the action of hemeenzymes such as peroxidases¹² and cytochrome P-450¹³⁻¹⁵ because of the support environment. Metalloporphyrin-immobilized molecular sieve presents many advantages such as replacement of molecular sieve as the protein portion of natural enzymes, providing a controlled steric environment for metalloporphyrins and serving as a model for the active site of cytochrome P-450. These systems show the chemoselectivity, regioselectivity and stereoselectivity in model reactions.¹⁶ Metalloporphyrin complexes immobilized into channels present particular properties through physical absorption due to the isolation of active sites, avoiding catalyst self-deactivation through dimerization and provide an easy way to recover them from the reaction media on suitable support materials.¹⁷⁻¹⁹ Other immobilization methods for epoxidation catalysts are the use of tetraphenylporphyrin manganese (III) chloride (Mn(TPP)Cl) supported on support-bound imidazole.^{20,21} This method avoids the use of co-catalyst imidazole.

To achieve the structural durable, steadily reusable catalysts for epoxidation remains a huge challenge. Among the various solid supports, HMS materials have attracted much attention, because they combine a high chemical and thermal stability with a crystalline structure formed by channels and cavities of strictly regular dimensions. A solution is based on the functionalized silica. Considering that amino-functionalized silica containing NH₂ units are capable of acting the combination of both NH₂ and support. Moreover, the soluble and redox properties of a metalloporphyrin-based hybrid are possibly tuned by inorganic blocks, thus it is possible to design a metalloporphyrin-based hybrid by combining the functionalized NH₂ with silica, so as to offer target hybrid catalysts with a good structural stability in solution, together with the higher redox activity for epoxidation.

In this study, amino-functionalized silica NH₂-HY, NH₂-

H β , NH₂-HMS were synthesized and manganese(III) 5-(4-carboxyphenyl)-10,15,20-triphenyl porphyrin chloride (Mn(TCPP)Cl) was designed to be grafted on these functionalized silica *via* amide bond. Thus obtained catalyst (Mn-NH-HY, Mn-NH-H β and Mn-NH-HMS) led to a heterogeneous epoxidation of alkenes, showing high conversion and selectivity, easy recovery and steady reuse. The final catalysts were fully characterized by XRD, ICP-AES, N₂ physisorption, SEM, TEM, FTIR and thermal analysis. Surface structure of catalysts had effect on the catalytic performance of grafted Mn(TCPP)Cl. A possible mechanism of pore structure which controls the diffusion of reactant and product molecules and surface hydrophobicity which facilitates adsorption of non-polar olefins and desorption of polar products was proposed to explain the enhanced catalytic activity for long-chain unsaturated compounds compared with homogeneous Mn(TCPP)Cl. The energy changes about formation of PorMnV=O species were also computationally calculated.

Experimental

Preparation of 5-(4-Carboxyphenyl)-10,15,20-triphenyl Porphyrin Catalyst (TCPPH₂). Salicylic acid (3.0 g), reagent grade benzaldehyde (4.6 g), 4-carboxy benzaldehyde (2.1 g) and dimethylbenzene (180 mL) were added to 250 mL neck flask. Freshly distilled pyrrole (2.7 g) and dimethylbenzene (20 mL) were added to the refluxing solution mixture in 5 min. After refluxing for 0.5 h, the solution was cooled to room temperature and was added in absolute ethanol. After a hot water wash, the resulting purple crystals were air dried, and finally dried in vacuum. Coarse product was purified by silica gel column chromatography using CHCl₃, 80% CHCl₃ and 20% carbinol as the eluting solvents.²²

Synthesis of Mesoporous Molecular Sieves. The formation of HMS solids depends on neutral assembly mechanism, involving hydrogen bonding between the neutral inorganic precursor and neutral amine surfactant.²³ HMS was synthesized following the procedures similar to those proposed *via* neutral templating pathway using dodecylamine (DDA) as the surfactant. 10 g of DDA was dissolved in 106 g of deionized H₂O and 78 g of ethanol under vigorous stirring. The surfactant solution was stirred for 15 min and then was slowly added in 42 g of tetraethyl orthosilicate (TEOS). The solution mixture was then stirred at 313 K for 0.5 h. The resultant solution was aged for 18 h at room temperature (25 °C) to obtain product. The solid precipitates were filtered out, dried at 100 °C over night, and calcined at 650 °C for 3 h. Finally, HMS was obtained for further experiments.

Synthesis of Silica Containing Amino Ligand. The obtained product was dispersed in dichloromethane and 2.00 g of (3-aminopropyl)triethoxysilane was added, then again brought to reflux for 16 h. After filtering, washing with dichloromethane, methanol and drying at 80 °C, silica containing amino ligands was obtained and denoted as NH₂-HY, NH₂-H β and NH₂-HMS.

Synthesis for Mn/HMS, Mn-NH-HY, Mn-NH-H β and Mn-NH-HMS. 0.1 g of TCPPH₂, 1 g of NH₂-HMS, 1 g of tetrahydrate manganese chloride and 150 mL of *N,N*-dimethylformamide (DMF) were added into a three-neck flask, then refluxed for 24 h. After cooling, washing with deionized water, and filtering, dichloromethane was used to extract the sample in a soxhlet extractor until no color was seen in the extracted solution and denoted as Mn-NH-HMS. The loading of Mn-NH-HMS was 62.4 mg/g-cat and the surface area of Mn-NH-HMS was 510 m²/g. Similarly, when Mn(TCPP)Cl was immobilized in NH₂-HY and NH₂-H β by using the above method, the product was designated Mn-NH-HY and Mn-NH-H β . The amount of adsorbed metalloporphyrin was determined by atomic emission spectroscopy with inductive coupled plasma (ICP-AES, Spectroflame-FVM03). The samples were digested by a traditional acid method (HF, HNO₃ and HCl, then H₃BO₃ was added to remove HF), diluted adequately and analysed for manganese.

0.1 g of Mn(TCPP)Cl in dichloromethane was slowly added to 1 g of mesoporous molecular sieve in 50 mL dichloromethane. The mixture was kept at 60 °C under magnetic stirring for 48 h. The solid product was then washed in a Soxhlet apparatus for 48 h in 300 mL dichloromethane until no presence of a board band at 480 nm, in order to remove the weakly adsorbed complexes on the mesoporous surface. Finally, the green solids were dried in air at 150 °C. The green colour of the samples obtained after thorough washings suggested the successful encapsulation of Mn(TPP)Cl inside the mesoporous materials. The product was designated Mn/HMS.

Measurement of Catalytic Performance. All of the reactions were carried out at room temperature under air in a 50 mL flask equipped with a magnetic stirrer bar. To a mixture of alkene (1 mmol), catalysts (the amount of Mn(TCPP)Cl was adjusted to 0.002 g), imidazole (2.8 mmol) and CH₃CN (10 mL) was added a solution of NaIO₄ (2 mmol) in H₂O (10 mL). The progress of reaction (oxidation of cyclooctene and cyclohexene) was monitored by GC. The catalyst was thoroughly washed with EtOH and hot water before reuse. In paper,²⁴⁻²⁶ the activity was defined as the amount of converted C=C double bond for the epoxidized methyl oleate and soybean oil. Selectivity was defined as desired product/all products. The conversion was monitored by the area decrease of the double-bond hydrogen signals which was at 5.4 ppm in the ¹H NMR spectra of epoxidized methyl oleate. The presence of signals between 50 and 60 ppm in the ¹³C NMR spectra was attributed to the epoxy carbons. So, the selectivity could be monitored by the area increase of the epoxy carbons signals between 50 and 60 ppm of the ¹³C NMR spectra of methyl oleate. Determination of oxidation efficiency is necessary to check how much oxidant is left after reaction. After reaction, the mixture is diluted by methanol. The mole of remaining oxidant can be determined by iodometric titration. A portion of the diluted methanol solution was added to H₂SO₄ aqueous solution containing potassium iodide and a small amount of starch. The mixture turned purple due to generation of I₂. Then, the mixture was

titrated with $\text{Na}_2\text{S}_2\text{O}_3$ aqueous solution until the color disappeared.

Characterization of Catalysts. The IR spectra were recorded on an ABB Bomem FTLA2000-104 spectrometer. X-ray power spectra were recorded using a Bruker D8-Advance diffractometer with $\text{Cu-K}\alpha$ radiation. ICP was recorded using a Spectroflame-FVM03. TG of the samples was recorded using a Mettler TGA/SDTA 851 E analyzer in the temperature range 25-900 °C at a heating rate of 20 °C/min. SEM measurements were performed on a CamScan CS44 scanning electron microscope. The samples for TEM observation were suspended in ethanol and supported on carbon-coated copper. The surface area (BET method) and average pore diameter (BJH method) were determined by N_2 adsorption-desorption method by a Micromeritics-ASAP 2020. The geometry optimizations of all intermediates and transition states were performed by using B3LYP functional and 6-31G basis set.

Results and Discussion

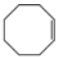
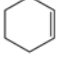
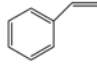
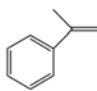
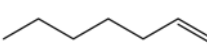
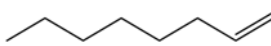
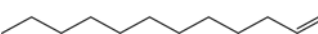
The effect of different oxidants on the epoxidation of cyclohexene catalyzed by Mn-NH-HMS was investigated in Table 1. NaIO_4 , H_2O_2 and TBHP (entries 2, 7 and 8) were chosen as oxygen source. The results showed that NaIO_4 was the best oxygen source because this oxidant, which was inert in the absence of catalyst, could give good oxidation of hydrocarbons with NaIO_4 catalyzed by grafted metalloporphyrin, imidazole played an important co-catalytic role. In recent research, NaIO_4 as the oxidizing agent showed special efficiency for different reactions, such as chemiluminescence reaction and oxidation reaction.²⁷⁻²⁹ Though H_2O_2 was inexpensive and easy to get, NaIO_4 was chosen as oxidant and used to investigate their catalytic activity and selected as the oxidizing agent for all the subsequent experiments. When the same reaction was carried out in the absence of imidazole, only small amounts of cyclohexene oxide were detected in the reaction mixture. NaIO_4 has poor ability to oxidize the cyclohexene without catalyst. No cyclooctene oxide was detected in the absence of oxidant in the reaction mixture either. The addition of imidazole to epoxidation reaction of cyclohexene, the yields increased to 92% at 24 h from 2%. The presence of imidazole was beneficial for these catalytic systems suggesting that it played a different role as a metal-ligand.³⁰ In the epoxidation, the mole ratio of oxidant: substrate was 2:1. So the conversion of each oxidant may be equal to or low compared with the conversion of substrate. The conversion of H_2O_2 was nearly 100% with a yield of 20% and unreacted H_2O_2 was not detected using above method after 24 h, which showed the oxidant efficiency was very low and large of oxidants with a low stability was decomposed. The conversion of NaIO_4 was 50-60% with a yield of 100% and there was about more than half amount of oxidant still unreacting with substrate. The conversion of TBHP was about 50% with a yield of 40%. From the results of defining the unreacted oxidants, the efficiency of NaIO_4 was the best and H_2O_2 was easily decomposed in this system.

Table 1. The catalytic performance of different catalysts for epoxidation of cyclohexene by NaIO_4 at room temperature^a

Entry	Catalysts	Reaction after 24 h		Reaction after 48 h	
		Conversion (%)	Selectivity (%)	Conversion (%)	Selectivity (%)
1	Mn-NH-HMS ^b	100	100	100	100
2	Mn-NH-HMS	92	100	100	100
3	Mn-NH-H β	76	100	100	100
4	Mn-NH-HY	54	100	100	100
5	Mn-NH-HMS no imidazole	2	100	2	100
6	No catalyst	0	0	0	0
7	Mn-NH-HMS ^c	20	100	22	100
8	Mn-NH-HMS ^d	40	94	42	94
9	Mn-NH-HMS ^e	44	100	72	100
10	Mn-NH-HMS ^f	34	100	43	100

^aReaction conditions: cyclohexene (1 mmol), catalysts (the amount of Mn(TCPP)Cl was adjusted to 0.002 g), imidazole (2.8 mmol) and CH_3CN (10 mL) was added a solution of NaIO_4 (2 mmol) in H_2O (10 mL). ^bcyclooctene instead of cyclohexene. ^c30% H_2O_2 instead of NaIO_4 aqueous solution. ^d65% TBHP instead of NaIO_4 aqueous solution. The by-products were allylic ketone. ^e methyl oleate instead of cyclohexene. ^fsoybean oil instead of cyclohexene.

Table 2. The catalytic performance of Mn-NH-HMS for epoxidation of other alkenes by NaIO_4 at room temperature^a

Entry	Alkenes	Conversion (%)	Selectivity (%)
1		100	100
2		92	100
3		76	76 ^b
4		80	74 ^c
5		86	100
6		19	100
7		12	100

^aReaction conditions: alkenes (1 mmol), catalysts (the amount of Mn(TCPP)Cl was adjusted to 0.002 g), imidazole (2.8 mmol) and CH_3CN (10 mL) was added a solution of NaIO_4 (2 mmol) in H_2O (10 mL). ^bThe by-products were benzaldehyde. ^cThe by-products were acetophenone.

Under the same reaction conditions a range of alkenes were oxidized in this catalytic system (Table 2). The obtained results showed that this catalyst was an efficient catalyst for alkene epoxidation. Increasing the length of linear alkenes led to lower epoxide yield and longer reaction times. The formation of epoxides for Mn-NH-HMS catalyst 24 h: 100% (cyclooctene), 92% (cyclohexene), 44% (methyl oleate, a

kind of fatty acid methyl esters), 34% (soybean oil, a kind of triglycerides). When cyclohexene was used as substrate for catalyst Mn-NH-HMS, it led to lower epoxide yield and longer reaction times. Angle strain at the double bond favoured activation of the olefin.³¹ The hoop tension of cyclooctene molecule was less than cyclohexene. Therefore, cyclooctene was easily epoxidized. HMS enhanced the catalytic performance of Mn(TCPP)Cl for substrate methyl oleate and soybean oil respect to homogeneous catalyst.³² The pore structure of HMS which controlled the diffusion of reactant and product molecules and surface hydrophobicity which facilitated adsorption of non-polar olefins and desorption of polar products played important roles on the oxidation activity.³³⁻³⁵ Grafted metalloporphyrin-catalyst also avoided their soluble, degradable characteristics and self-deactivation through dimerization. The pore structure of HMS offered target support with good structural stability in solution and enhanced the catalytic performance. So, the yield of heterogeneous Mn-NH-HMS catalyst with methyl oleate and soybean oil as substrates was higher than yield of homogeneous catalyst. Soybean oil revealed the effectivity of catalyst. When soybean oil was used as substrate for catalyst Mn-NH-HMS, the epoxides were 34% at 24 h (entry 10). According to its stereochemical structure that olefinic chains in triglyceride molecules containing more than 18 carbon atoms, the dynamic diameter of methyl oleate molecule was less than soybean oil. Therefore, methyl oleate was easily epoxidized because of its steric hindrance. The results also showed increasing the length of hydrocarbon chain led to lower epoxide yield and longer reaction times. It meant that the structure of HMS was sensitive to the chain length and showed a good selectivity towards alkenes.

With the epoxidation of cyclohexene by NaIO₄ in presence of imidazole as a model reaction, catalytic performances of Mn-NH-HY, Mn-NH-H β and Mn-NH-HMS catalysts were listed in Figure 1. Mn-NH-HY, Mn-NH-H β and Mn-NH-HMS catalysts caused a liquid-solid heterogeneous epoxidation system, and exhibited an excellent conversion with high selectivity. The conversion was found to increase with

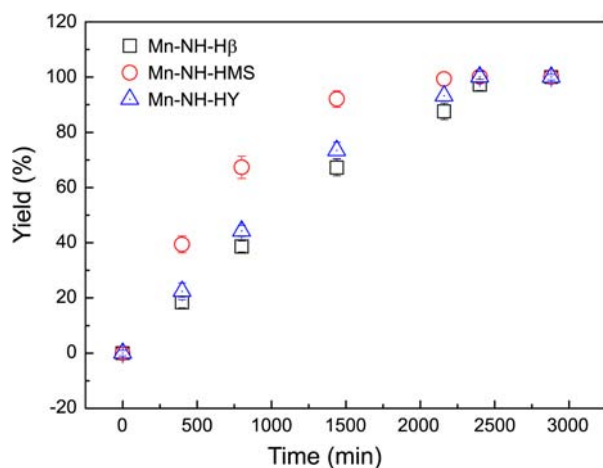


Figure 1. Catalytic performance of different heterogeneous catalysts for epoxidation of cyclohexene by NaIO₄.

Table 3. Adsorption average pore diameter a_0 and content of grafted metalloporphyrin, specific surface areas and cumulative pore volumes of supports before and after loading with Mn(TCPP)Cl

Samples	Mn(TCPP)Cl content (mg/g)	Org content (mmol/g)	a_0 (nm)	S_{BET} (m ² /g)	Cumulative pore volume (cm ³ /g)
HMS	-	-	2.10	821	0.43
HY	-	-	-	583	-
H β	-	-	-	445	-
NH ₂ -HMS	-	0.874	2.02	547	0.29
NH ₂ -HY	-	0.646	-	336	-
NH ₂ -H β	-	0.634	-	216	-
Mn-NH-HMS	62.4	-	2.07	510	0.28
Mn/HMS	12.7	-	2.39	492	0.30
Mn-NH-HY	16.3	-	-	280	-
Mn-NH-H β	14.6	-	-	198	-

increasing time. In the presence of Mn-NH-HY, Mn-NH-H β and Mn-NH-HMS almost same trend was observed, but Mn-NH-H β and Mn-NH-HMS took little longer time to reach complete conversion than Mn-NH-HMS. As seen in Figure 1, the percent reaction rate followed the order: Mn-NH-H β < Mn-NH-HY < Mn-NH-HMS. The mesoporous support played a major role in epoxidation due to its higher surface area. The higher surface area could also reduce the energy barrier and more active center reacted with cyclohexene. The order of surface area was in good agreement with the order of reaction rate. Higher surface area was beneficial to the conversion. Upon grafted with Mn(TCPP)Cl, the activity increased remarkably in the epoxidation reactions. This showed that the epoxidized activity was associated with Mn(TCPP)Cl grafted on molecular sieve. No catalytic activity was observed in the reaction solution after removal of catalyst by filtration (in a run where oxidant still remained), confirming that the catalytic reaction was heterogeneous. The carrier of different crystal forms also affected the mole ratio between organic functional groups and Mn(TCPP)Cl. The ratio followed the order: Mn-NH-H β (39:1) \approx Mn-NH-HY (36:1) < Mn-NH-HMS (14:1) according to Table 3. The silanol groups (\equiv Si-OH), always present in silica gel, are responsible for the adsorption of organic molecules; these OH groups are mainly placed on HMS internal surface that represent the main contribution to the total surface area of the porous material. Luan *et al.* suggested that abundant silanol groups on the inner surface of mesopores serve as the sites for grafting functional groups during the surface modification.³⁶ HMS which was modified with NH₂ exhibited a reduction in surface area, pore size and total pore volume. Pristine HMS exhibited a BET surface area of 821 m²/g, pore volume of 0.43 cm³/g, and pore size at 2.1 nm. Surface functionalization resulted in an apparent decrease in these textural parameters in Figure 2, which could be attributed to the immobilization of organic functional groups on the inner wall of mesopores. The isotherm can be classified as a type IV. Adsorption isotherm of the encapsulated catalysts showed three well-distinguished regions: mono and multilayer

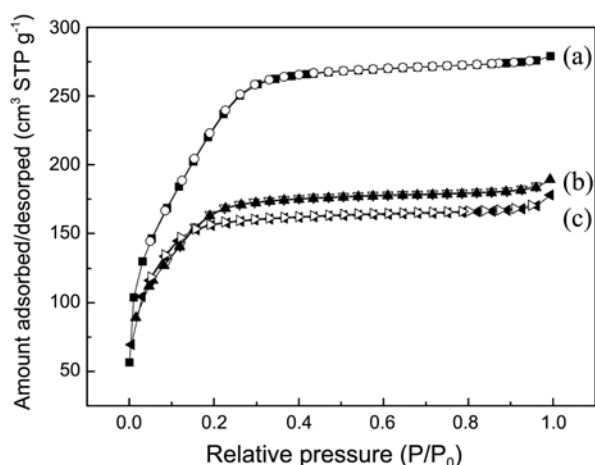


Figure 2. Nitrogen adsorption/desorption isotherms for (a) HMS; (b) NH₂-HMS; (c) Mn-NH-HMS.

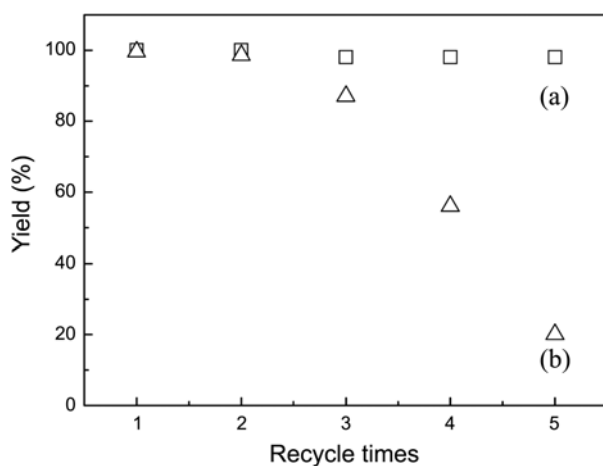


Figure 3. Data for catalytic efficiency for (a) reused Mn-NH-HMS catalyst and (b) reused Mn/HMS catalyst with NaIO₄ as oxidant.

adsorption on the pore walls, capillary condensation, and multilayer adsorption on the outer surface. The size of metalloporphyrin is about 1.0 nm. It was expected that spread of Mn(TCPP)Cl occurred without spatial strain, which meant more NH₂ groups reacting with it. The catalytic efficiency of catalysts was related to the structure which was also reflected by data of characterization.

Mn-NH-HMS and Mn/HMS were separated by centrifugation and washed by ethanol and dichloromethane after the first use. The obtained catalysts were reused after being dried in air. Figure 3 displayed the stability and possible reuse. At first-run, the conversion of cyclohexene reached 100%, and the selectivity of epoxides was 100% for Mn-NH-HMS. The utility of Mn-NH-HMS catalyst for repeated use was tested, and the catalytic activity remained 98% when the catalyst was employed for the five times. When Mn/HMS catalyst was recycled five times, its catalytic performance decreased to 20%. In addition, from ICP, it was found that the amount of manganese ion of the Mn-NH-HMS catalyst after the reaction was generally consistent with that of manganese ion of the fresh catalyst on the

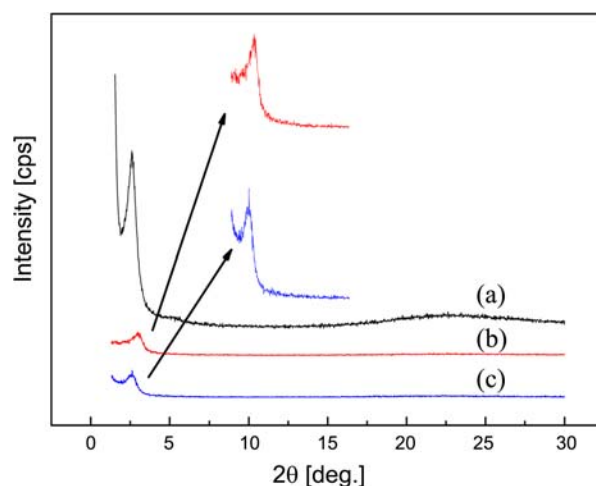


Figure 4. XRD patterns of (a) HMS; (b) NH₂-HMS; (c) Mn-NH-HMS.

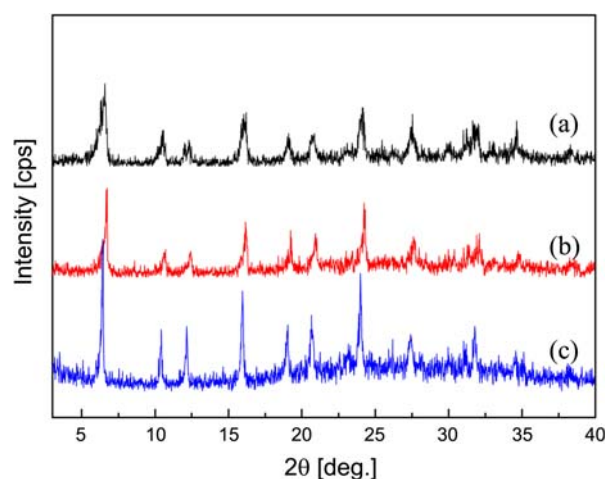


Figure 5. XRD patterns of (a) HY; (b) NH₂-HY; (c) Mn-NH-HY.

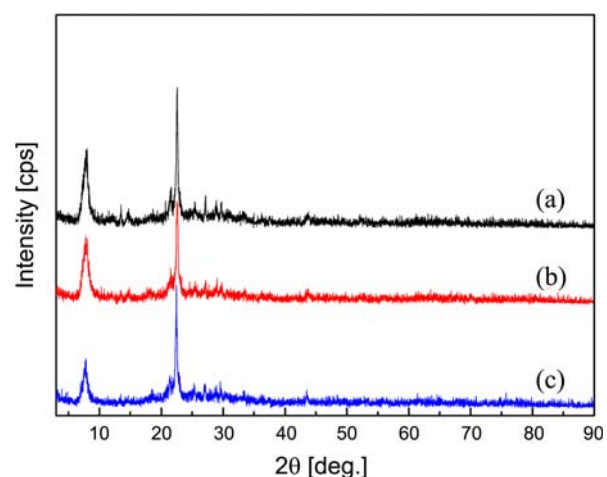


Figure 6. XRD patterns of (a) Hβ; (b) NH₂-Hβ; (c) Mn-NH-Hβ.

whole. One leaching test (heterogeneity of the catalyst) for the catalyst has also been performed. 0.5 wt % of catalytic center (Mn(TCPP)Cl) leached from the support after five times. Mn-NH-HMS exhibited a good structural stability in

solution, together with the higher redox activity for epoxidation compared with Mn/HMS. The results for the recycling test were also good for Mn-NH-H β and Mn-NH-HY just with longer time.

The XRD power patterns measured for HMS, NH₂-HMS and Mn-NH-HMS were shown in Figure 4. All samples exhibited a single low-angle (100) peak and an excellent long range order, characteristic of wormhole mesopores structure. In addition, the intensity of d_{100} reflection of NH₂-HMS and Mn-NH-HMS decreases and d_{100} spacing shifted to a higher angle, compared with HMS. This phenomenon suggested a decrease in uniformity of the porous structure because of the organic functional groups and Mn(TCPP)Cl incorporation. The pore volume was decreased from 0.43 cm³/g for HMS to 0.28 cm³/g for Mn-NH-HMS. This result indicated that the internal pores of Mn-NH-HMS were occupied by the Mn(TCPP)Cl complex. The distribution of spacing became narrower in Figures 5 and 6 because of larger crystallite dimension after grafted with Mn(TCPP)Cl. No any crystalline phase of Mn(TCPP)Cl species was observed. Mn(TCPP)Cl was highly dispersed on support. The XRD data also showed that the crystallinity of HY and H β zeolite was maintained after preparation of NH₂-HY, NH₂-H β , Mn-NH-HY, Mn-NH-H β , indicating that no obvious framework collapse associated with the preparation procedure and no organic functional groups or Mn(TCPP)Cl were grafted on the inner wall of pores. So Mn(TCPP)Cl was really grafted outside the pores for support HY and H β . SEM analysis was carried out to better understand the catalysts' morphology. The spheres of Mn-NH-H β , Mn-NH-HY and Mn-NH-HMS samples were shown in Figure 7. The morphology of Mn-NH-HY and Mn-NH-H β was quite different from Mn-NH-HMS. Mn-NH-H β showed clouds resembling particle and some agglomerates have been detected. Figure 7(c) clearly demonstrated that the spherical morphology of the silica particles was retained during the synthesis Mn-NH-HMS spheres. According to the BET results, Mn-NH-HMS exhibited a higher surface area than the other two samples. So Mn-NH-HMS revealed large amount of mesopores at the

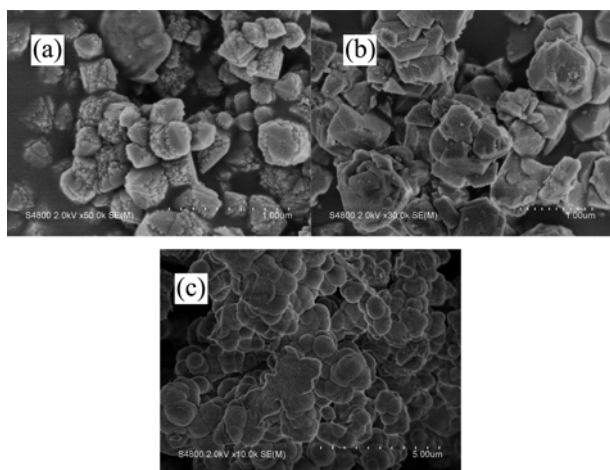


Figure 7. SEM pictures of (a) Mn-NH-HY; (b) Mn-NH-H β ; (c) Mn-NH-HMS.

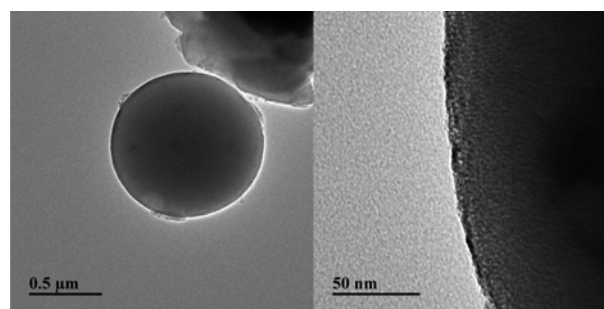


Figure 8. TEM images of Mn-NH-HMS.

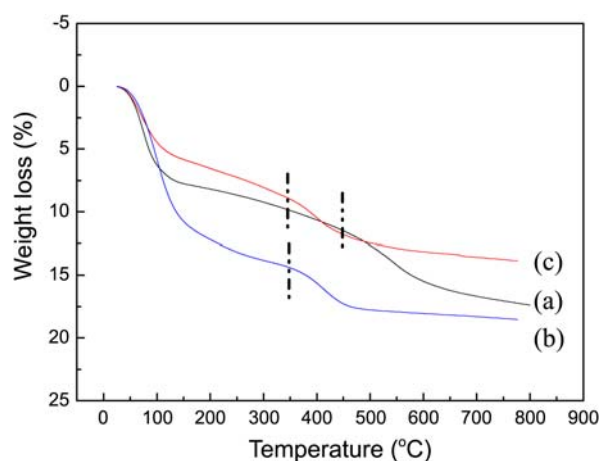


Figure 9. TG/DTG curves for (a) NH₂-HMS; (b) NH₂-H β ; (c) NH₂-HY.

internal region. The XRD results were in good agreement with the results from results of BET, SEM and TEM (Figure 8).

Further investigation using TG/DTG curves (Figure 9) showed that the organic functional groups grafted on silica were stable up to 447 °C for HMS (Figure 9(a)), 345 °C for H β (Figure 9(b)) and 339 °C for HY (Figure 9(c)) calculated by the derivation of weight loss, respectively. After grafted on mesoporous molecular sieve, an increase on the decomposition temperature was observed. This process produced

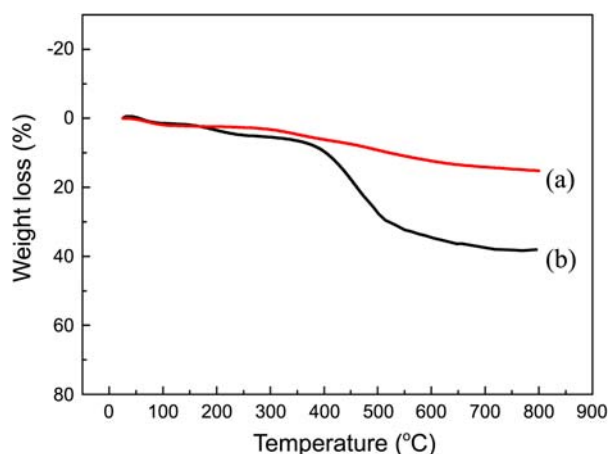


Figure 10. TG/DTG curves for (a) Mn(TCPP)Cl; and (b) Mn-NH-HMS.

an increase of almost 100 °C on the stabilization of organic functional groups than other samples. The TG/DTG analysis of Mn(TCPP)Cl was also determined. As shown in Figure 10(b), a significant weight loss step appeared at the temperature range of 362-511 °C, which was attributed to the decomposition of porphyrin rings. For the sample Mn-NH-HMS (Figure 10(a)), between 25 °C-150 °C with a lost weight corresponding to water physically adsorbed, between 257 °C-418 °C with a lost weight assigned to the traces of the DMF, between 418 °C-667 °C with a lost weight due to the condensation of Mn(TCPP)Cl and organic functional groups (-CH₂-CH₂-CH₂-NH). That Mn(TCPP)Cl and organic functional groups (-CH₂-CH₂-CH₂-NH) were present on HMS internal surface resulted to their increase in the thermal decomposition reaction activation energy.

In order to gain sight of these heterogeneous catalysts, FTIR spectroscopies were used. The FTIR spectra of 5-(4-carboxyphenyl)-10,15,20-triphenyl porphyrin (TCPPH₂), Hβ, NH₂-Hβ, Mn-NH-Hβ were shown in Figure 11. The bands observed at 798 (Si-O), 1098 (Si-O-Si) and 1250 (Si-O-Si) cm⁻¹, respectively, were the main features of Hβ. The bands at 1080 and 1250 cm⁻¹, which could be ascribed to the Si-O-Si stretching vibration, significantly increased with the existence of Si from NH₂. The bands observed at 1384 cm⁻¹ for B, C and D could be ascribed to the C-H stretches of silane. Due to the metalloporphyrins highly grafted on support, the main characteristics of the immobilized complexes (absorption at 1688 cm⁻¹ (C=O) for TCPPH₂) could not be observed. The presence of abroad inconspicuous band at 2960 cm⁻¹, which was characteristic of the asymmetric vibration of the CH₂ groups, further confirms the successful silylation.³⁷ In the hydroxyl region, the weak band at 1633 cm⁻¹ and the broad band at 3450 cm⁻¹ could be attributed to a combination of the stretching vibration of cross hydrogen-bonding interactions and the H-O-H stretching mode of physisorbed water.

In most cases, their catalytic behavior was believed to derive from the high-valent manganese(V)-peroxide porphy-

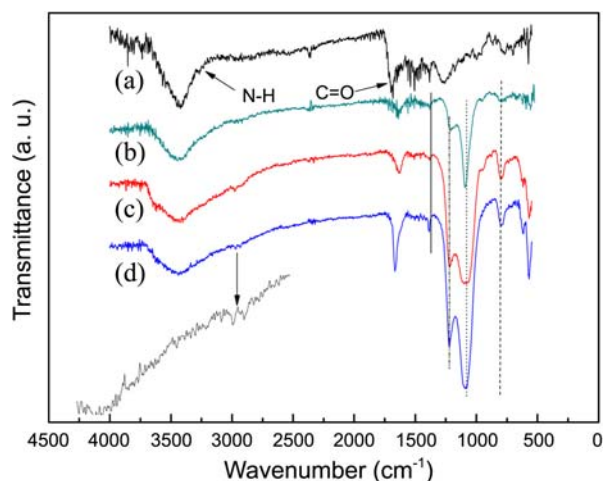


Figure 11. FT-IR spectra of: (a) TCPPH₂; (b) Hβ; (c) NH₂-Hβ; (d) Mn-NH-Hβ.

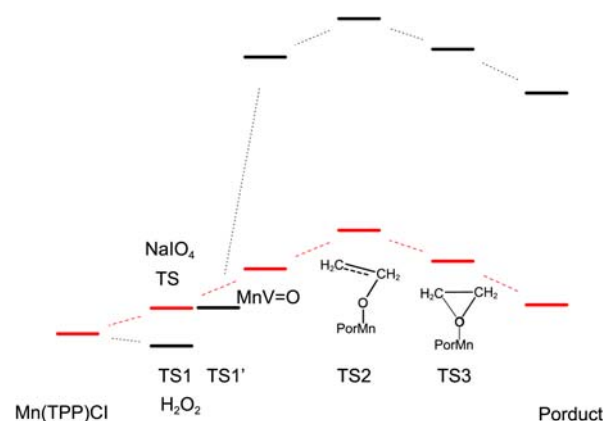


Figure 12. Energy profiles for epoxidation of alkenes by NaIO₄ and H₂O₂.

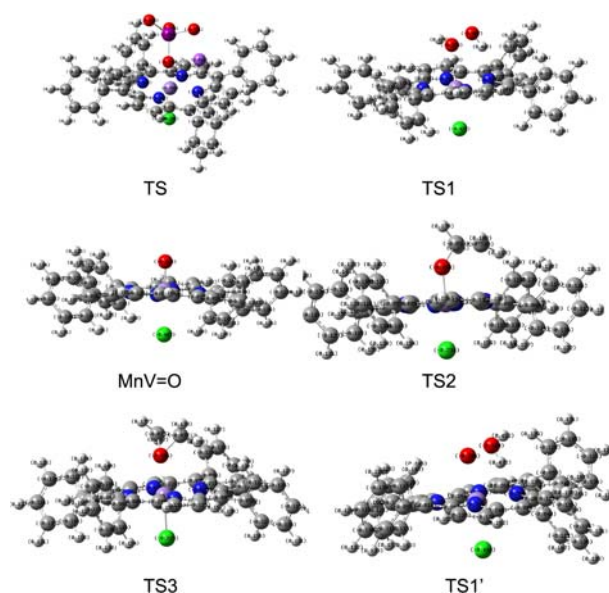


Figure 13. Optimized geometries for the catalyst species.

rin species. The formation of PorMnV=O species was responsible for catalytic activity of manganese porphyrins. It seemed that oxygen atom transfer from NaIO₄ or H₂O₂ to manganese had occurred to generate a Mn(V)-oxo complex. PorMnV=O species supported the improvement of the epoxidation performance. A energy pathway has been identified, which started with the activation of NaIO₄ or H₂O₂ to form porMnV=O. Therefore, the first step of our investigation was an analysis of the coordination and activation of the oxidant. The energy profile was shown in Figure 12, and the optimized geometries of the key species were given in Figure 13. The energy of TS1 for oxidant H₂O₂ was lower than both catalyst and oxidant. The coordination between H₂O₂ with Mn(TPP)Cl was spontaneous reaction, while the formation of TS needed energy to be activated. There was a difference between H₂O₂ and NaIO₄ for the formation of MnV=O. Formation of TS1' from TS1 was a proton of H₂O₂ transfer process. So for oxidant H₂O₂ more energy was used to activate the proton-transfer process. Energy barrier existed at the formation of TS2 for both reactions. From the results

of Figure 12 and the activity performance using different oxidants, yield results for different oxidant NaIO₄ (100% yield) or H₂O₂ (20% yield) were consistent with the step being the formation of the TS2. More energy was needed for H₂O₂ compared with NaIO₄.

Conclusion

The main goal of this present study was to combine the metalloporphyrin synthesis and the surface modification technique to obtain materials with achieving the structural durable, steadily reusable catalysts for epoxidation. XRD, ICP-AES, N₂ physisorption, SEM, TEM, FTIR and thermal analysis were employed to analyse these heterogeneous materials. HMS after being grafted with Mn(TCPP)Cl revealed promising properties respect to HY and H β . The possible mechanism of HMS as promoter was proposed to understand that the grafted Mn(TCPP)Cl catalysts have shown better catalytic performance. The energy changes about epoxidation of alkenes by NaIO₄ and H₂O₂ proved the efficiency of NaIO₄.

Acknowledgments. This work was supported financially by the National "Twelfth Five-Year" Plan for Science & Technology (2012BAD32B03), the National Natural Science Foundation of China (20903048) and the Academy and Research Institutes (BY2010118) in Jiangsu Province of China.

References

- Biermann, U.; Friedt, W.; Lang, S. *Angew. Chem. Int. Ed.* **2000**, *39*, 2206.
- Kumar, D.; Ali, A. *Energy Fuels* **2012**, *26*, 2953.
- Ye, X.; Jiang, P. P.; Zhang, P. B.; Dong, Y. M. *Catal. Lett.* **2010**, *137*, 88.
- Cho, S. H.; Walther, N. D.; Nguyen, S. T.; Hupp, J. T. *Chem. Commun.* **2005**, 5331.
- Huang, G.; Luo, Z. C.; Xiang, F.; Cao, X.; Guo, Y. A.; Jiang, Y. X. *J. Mol. Catal. A: Chem.* **2011**, *340*, 60.
- Figueira, F.; Cavaleiro, J. A. S.; Tome, J. P. C. *J. Porphy. Phthalocya.* **2011**, *15*, 517.
- Holland, B. T.; Walkup, C.; Stein, A. *J. Phys. Chem. B* **1998**, *102*, 4301.
- Costa, A. A.; Ghesti, G. F.; Macedo, J. L.; Braga, V. S.; Santos, M. M.; Dia, J. A.; Dias, S. C. L. *J. Mol. Catal. A: Chem.* **2008**, *282*, 149.
- Silva, M.; Azenha, M. E.; Pereira, M. M.; Burrows, H. D.; Sarakha, M.; Forano, C.; Ribeiro, M. F.; Fernandes, A. *Appl. Catal. B: Environ.* **2010**, *100*, 1.
- Moghadam, M.; Tangestaninejad, S.; Mirkhani, V.; Mohammadpoor-Baltork, I.; Moosavifar, M. *J. Mol. Catal. A: Chem.* **2009**, *302*, 68.
- Gao, B. J.; Wang, R. X.; Zhang, Y. *J. Appl. Polym. Sci.* **2009**, *112*, 2764.
- Brien, P. J. O. *Chem. Biol. Interact.* **2000**, *129*, 113.
- Kellner, D. G.; Hung, S. C.; Weiss, K. E.; Sligar, S. G. *J. Biol. Chem.* **2002**, *277*, 9641.
- Yoshioka, S.; Tosha, T.; Takahashi, S.; Ishimori, K.; Hori, H.; Morishima, I. *J. Am. Chem. Soc.* **2002**, *124*, 14571.
- Ferreira, A. D. Q.; Vinhado, F. S.; Iamamoto, Y. *J. Mol. Catal. A: Chem.* **2006**, *243*, 111.
- Serwicka, E. M.; Połtowicz, J.; Bahrnowski, K.; Olejniczak, Z.; Jones, W. *Appl. Catal. A: Gen.* **2004**, *275*, 9.
- Vinhado, F. S.; Prado-Manso, C. M. C.; Sacco, H. C.; Iamamoto, Y. *J. Mol. Catal. A: Chem.* **2001**, *174*, 279.
- Iamamoto, Y.; Ciuffi, K. J.; Sacco, H. C.; Prado, C. M. C.; Moraes, M.; Nascimento, O. R. *J. Mol. Catal.* **1994**, *88*, 1676.
- Saikia, L.; Srinivas, D. *Cata. Today* **2009**, *141*, 66.
- Moreira, M. S. M.; Martins, P. R.; Curi, R. B.; Nascimento, O. R.; Iamamoto, Y. *J. Mol. Catal. A: Chem.* **2005**, *233*, 73.
- Moghadam, M.; Tangestaninejad, S.; Mirkhani, V.; Kargar, H.; Komeili-Isfahani, H. *Catal. Commun.* **2005**, *6*, 688.
- Adler, A. D.; Longo, F. R.; Kampas, F. *J. Inorg. Nucl. Chem.* **1970**, *32*, 2443.
- Tanev, P. T.; Pinnavaia, T. J. *Sci.* **1995**, *267*, 865.
- Jiang, P. P.; Chen, M.; Dong, Y. M.; Lu, Y.; Ye, X.; Zhang, W. J. *J. Am. Oil. Chem. Soc.* **2010**, *87*, 83.
- Miyake, Y.; Yokomizo, K.; Matsuzaki, N. *J. Am. Oil. Chem. Soc.* **1998**, *75*, 15.
- Gunstone, F. D. *J. Am. Oil. Chem. Soc.* **1993**, *70*, 1139.
- Zhuang, Y.; Cao, G.; Ge, C. *Spectrochim. Acta Part A: Mol. Biomol. Spectrosc.* **2012**, *85*, 139.
- Tabatabaeian, K.; Mamaghani, M.; Mahmoodi, N. O.; Khorshidi, A. *Catal. Commun.* **2008**, *9*, 416.
- Kim, S.; Chung, J.; Kim, B. M. *Tetrahedron Lett.* **2011**, *52*, 1363.
- Moghadam, M.; Tangestaninejad, S.; Habibi, M. H.; Mirkhani, V. *J. Mol. Catal. A: Chem.* **2004**, *217*, 9.
- Bhattacharjee, S.; Anderson, J. A. *J. Mol. Catal. A: Chem.* **2006**, *249*, 103.
- Du, G. D.; Tekin, A.; Hammond, E. G.; Woo, L. K. *J. Am. Oil. Chem. Soc.* **2004**, *81*, 477.
- Wang, J.; Xu, L.; Zhang, K.; Peng, H.; Wu, H.; Jiang, J.; Liu, Y.; Wu, P. *J. Catal.* **2012**, *288*, 16.
- Cheneviere, Y.; Chieux, F.; Caps, V.; Tuel, A. *J. Catal.* **2010**, *269*, 161.
- Zhao, Z.; Liu, Y.; Wu, H.; Li, X.; He, M.; Wu, P. *J. Porous Mater.* **2010**, *17*, 399.
- Luan, Z. H.; Fournier, J. A.; Wooten, J. B.; Miser, D. E. *Micropor. Mesopor. Mater.* **2005**, *83*, 150.
- Joseph, T.; Kumar, K. V.; Ramaswamy, A. V.; Halligudi, S. B. *Catal. Commun.* **2007**, *8*, 629.